Alexandria Engineering Journal (2010) 49, 357–370

Alexandria University

Alexandria Engineering Journal

www.elsevier.com/locate/aej
www.sciencedirect.com

ORIGINAL ARTICLE

Behavior of stub girder floor system with partial shear connection

El-Sayed Mashaly [a], Hesham ZienEldin [a], Mohamed El-Heweity [a,*], Raafat Ismail [b], Howida Ismail [a]

[a] *Department of Structural Engineering, Faculty of Engineering, Alexandria University, Alexandria, Egypt*
[b] *Department of Engineering Mathematics and Physics, Faculty of Engineering, Alexandria University, Alexandria, Egypt*

Received 7 December 2009; accepted 21 June 2010
Available online 26 January 2011

KEYWORDS

Composite structures;
Floor systems;
Steel girders;
Stubs;
Shear connectors

Abstract A stub-girder floor system is a composite system constructed from a continuous steel beam and a reinforced concrete slab separated by a series of short, typically wide, flange sections called stubs. The finite element method has been used in the analysis of this composite system where it is capable to represent the constituent parts, adopt adequate elements and use appropriate solution techniques. As the behavior of stub-girders presents significant nonlinear effects, it is fundamental that the interaction of all different components should be properly modeled as well as the interface behavior. The present work focuses on the modeling of stub-girders with full and partial shear connection in two and three dimensions. The proposed model contains all the main structural parameters and their associated nonlinearities (concrete slab, steel beam, stubs, and shear connectors). In this model, the shear connectors are modeled as springs to consider the geometry of studs in addition to the nonlinearity due to the interaction between the shear connector and the concrete slab. Tests and numerical results available in the literature are used to validate the models. Based on

* Corresponding author.
E-mail addresses: elsayedmashaly@yahoo.com (E.-S. Mashaly), heshamzieneldin@yahoo.com (H. ZienEldin), heweity@hotmail.com (M. El-Heweity), raafati@yahoo.com (R. Ismail), howida@gmail.com (H. Ismail).

Peer review under responsibility of Faculty of Engineering, Alexandria University.
doi:10.1016/j.aej.2010.06.001

Production and hosting by Elsevier

the proposed finite element model, an extensive parametric study of stub-girders is performed, considering the material properties, relative dimensions and shear connector characteristics, where valuable recommendations and conclusions are achieved.

1. Introduction

The stub-girder floor system, shown in Fig. 1, is one of the structural methodologies that attempts to minimize floor-to-floor heights by incorporating services within the structural depth. The use of the stub girder floor system generally reduces the amount of structural steel in the floor system by about 25%, and the total cost of the floor system by about 15% [17,6].

Few researches [9,10] related to the investigation of different parameters that could control the behavior of stub girder floor system were found. In these researches, some parameters such as the effect of type of loading, stub location and height of stub were investigated.

For the analysis of stub girder system, Colaco [7] utilized a vierendeel modeling scheme for the stub girder to arrive at a set of stress resultants, which in turn were used to size the various components. Harbok and Hosain [8] developed a computer program based on the method of substructures to get the deflection of stub girders, based on an assumption of full interaction between the concrete slab and the stubs. Other studies have examined approaches such as non prismatic beam analysis, but it is not accurate as the vierendeel approach, since it tends to overlook some important local effects and overstates the service load deflections [3,19]. Madros [13] presented a simple linear analytical method for analyzing the stub-girder system based on partial-interaction concept under uniform load. The method treated the stub-girder as a beam with three distinct layers, which is called the layered beam model. The top and bottom layers behaved according to the normal beam bending theory, while the middle layer was a shear layer without any bending stiffness. At the interface between the steel and concrete elements, the headed stud shear connectors were modeled as linear elastic built in cantilevers. The method therefore smeared the effects of all the contributing elements. Comparison of these results with the experimental and numerical results gave good agreements within elastic range. Wang et al. [18] presented two different methods to determine the ultimate load-carrying capacity of stub girders, where full interaction was assumed between the concrete slab and the stubs. In the first method, the stub girder is modeled as a vierendeel truss girder. Based on an assumed collapse mechanism, an explicit expression to calculate the ultimate load is derived. The second method used the finite-element software package ABAQUS for nonlinear analysis of idealized two-dimensional stub girder models. The two methods furnish results that are in reasonable agreement with experimental results, for girders in which the premature failure of shear connectors, the local buckling of stubs and the main girder, and the longitudinal shear failure are prevented. Based on the elastic analytical model presented by Madros [13], the work was extended by Kasem [11] and Ismail et al. [9,10] through developing a program called "PZA". The analysis was in accordance with the plastic zone theory to consider the material nonlinearity assuming a linear stud connector slip response.

The PZA was used to analyze three full composite stub-girders SG5, SG6, and SG7 given by Wang et al. [18]. The results of program PZA were in good agreement with the experimental results. The PZA program was used to study different parameters such as the shear connector diameter and the stub height. Moreover, Kasem [11] and Ismail et al. [9,10] used the finite element method to analyze two stub-girders. In the first girder, full composite stub-girder, SG7, a full interaction between the concrete slab and the stubs was assumed [18]. In the second girder, BJOR, as reported by Madros [13], the shear studs were modeled by elastic–plastic beam element to consider the partial interaction between the concrete slab and the stubs. The results obtained from the finite element program, COSMOS, are in relatively close agreement with the experimental values for both full composite girder, SG7, and partial composite girder, BJOR. Also the finite element program was used to study different parameters such as the type of loading, stub locations and smearing of stubs.

In this study, a finite element model is utilized in the analysis of the stub-girder floor system. The work focuses on the modeling of stub-girders with full and partial shear connection in two and three dimensions. The proposed model implements all the main structural parameters and their associated nonlinearities (concrete slab, steel beam, stubs and shear connectors). In this model the shear connectors are modeled as springs to consider the geometry of studs in addition to the nonlinearity due to the interaction between the shear connector and the concrete. Tests and numerical results available in the literature are used to validate the models. Based on the validated finite

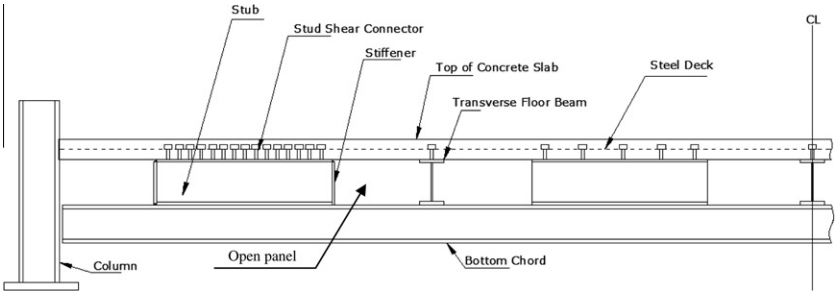

Figure 1 Components of stub girder floor system.

element model, an extensive parametric study of stub-girders is performed, considering the material properties, relative dimensions and shear connector characteristics, where valuable recommendations and conclusions are achieved.

2. Finite element modeling of stub girder floor system

In this study, the finite element package ANSYS [2] is used in the analysis. Two- and three-dimensional finite element models are proposed and examined.

2.1. Two-dimensional model of stub girder (2D model)

2.1.1. Finite element types

2D element (PLANE42) which is suitable for plane stress analysis is used to model all steel components and the concrete slab. The thicknesses of the plane stress elements assigned are equal to the effective width of the concrete slab, flange widths and web thicknesses of the steel sections as appropriate. Two cases of composite action for stub girders were simulated. The first case, a full composite action for stub girders, is achieved by gluing the area of the slab concrete and the areas of the stub flanges. In the second case, partial composite action is considered for the stub girder by modeling the studs with nonlinear spring elements (COMBIN39) represented by the load–slip curve of studs [12] (Fig. 2). Elastic beams (BEAM3) are used under the concentrated loads and over the supports to avoid local yielding. Typical finite element meshes of the stub girders for the two cases of composite action are shown in Figs. 3 and 4.

2.1.2. Material modeling

The von Mises yield criterion with isotropic hardening rule is used to model the steel components. The steel stress–strain relationship is elastic–perfectly plastic. The compressive behavior of the concrete slab is modeled by a multilinear isotropic hardening relationship [5], which uses the von Mises yield criterion. The resulting assumed constitutive relations of the concrete and steel are shown in Fig. 5. Where, for steel, f_s, ε_s, f_{sy}, ε_s, and E_s are steel stress, steel strain, yield steel stress, yield steel strain, and steel modulus of elasticity, respectively. While, for concrete, f_c, f'_c, f'_t, ε'_c, ε_u, ε'_t, and ε_0, are concrete strength in compression, unconfined concrete strength, ultimate tensile concrete strength, unconfined concrete strain, ultimate strain, ultimate tensile strain, and zero strain, respectively.

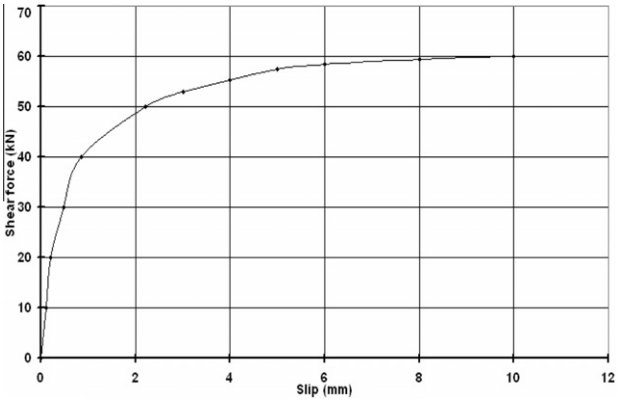

Figure 2 The proposed load–slip curve [8].

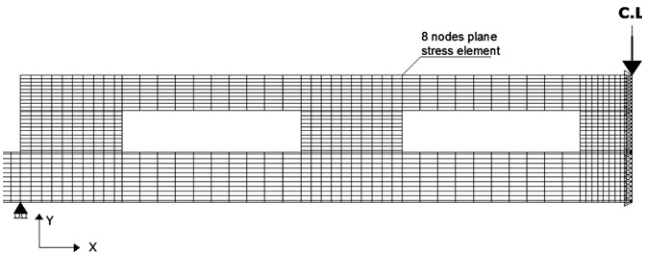

Figure 3 Finite element mesh for stub girder with full composite action.

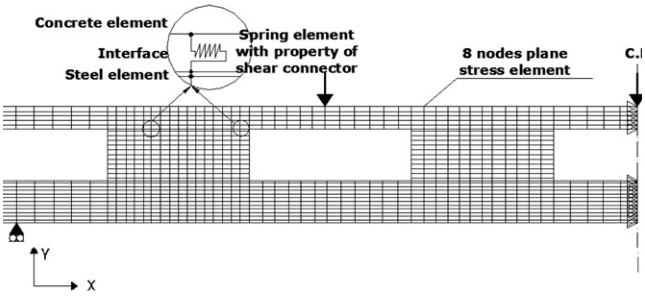

Figure 4 Finite element mesh for stub girder with partial composite action.

2.1.3. Application of loads and numerical control

The load is incrementally applied to the stub girders with full composite action, utilizing the displacement control method to overcome divergence problems where there is only one load at the mid-span (Fig. 3). On the other hand, in the stub girder with partial connection the load control method is used where three equal concentrated loads are applied incrementally with no direct relationship between the displacements at the three applied loads, as shown in Fig. 4. It is worth noting that divergence and shear connector failure (by monitoring the shear force at studs) are used as the failure criteria to define the ultimate load.

2.1.4. Boundary conditions

For partial interaction modeling, the transfer of stresses from the concrete slab to the top flanges of the stubs can be achieved by coupling every pairs of coincident nodes at the interface in the *y*-direction only while in *x*-direction spring elements are used between these coincident nodes. This arrangement allows slip but prevents overlapping or uplifting between the concrete slab and stubs. The node at the support was restricted from moving in the *y*-direction while all nodes along the surface of the stub girder at the mid-span were restricted from moving in the *x*-direction due to symmetry, where half of stub girder is analyzed.

2.2. Three-dimensional model of stub girder with partial shear connection (3D model)

A 3D model is used to represent the stub girder with partial shear connection which was tested by Bjorhovde and Zimmerman [3].

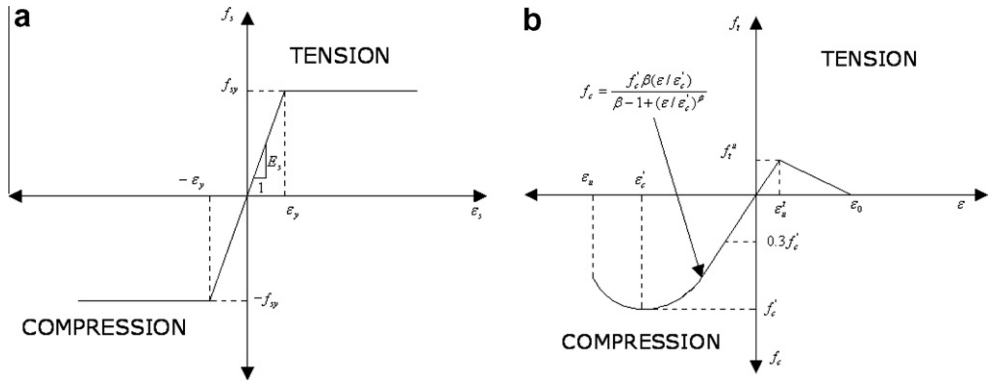

Figure 5 Idealized uniaxial stress–strain relationships. (a) Steel and (b) concrete.

2.2.1. Finite element types

The types of finite elements used are chosen from the library of software package ANSYS [2]. Elasto-plastic shell element (SHELL43), elastic element (SHELL63) and solid element (SOLID65) are used to model the steel sections, the profiled steel sheet, and the concrete slab, respectively, while nonlinear spring elements (COMBIN39) are used to model the shear connectors. Both longitudinal and transverse reinforcement bars are modeled as smeared throughout the solid finite element (SOLID65). The elastic shell element (SHELL63) is used to model the stiffener over the support while elastic beam element (BEAM3) is used under the concentrated loads throughout the concrete slab depth to avoid local yielding. The load–slip curve for the headed studs, obtained from the push-off tests [12], and the actual number and spacing used in the experiment are utilized in the analysis.

2.2.2. Material modeling

Material modeling is taken as described in the 2D model but the tensile behavior of the concrete and consequently the crack failure are taken into consideration, where $f_t^u/f_c' = 0.1$. Moreover, the concrete element shear transfer coefficient is considered as 0.2 for open crack and 0.6 for closed crack [2].

During this study and previous studies [14–16], it has been found that if the crushing capability of the concrete is turned on (the elastic modulus is set to zero in all directions so the element effectively disappears), the finite element models fail prematurely where the crushed concrete elements significantly reduce the local stiffness. Finally, the model showed a large displacement, and the solution diverged. Therefore, in this study, the crushing capability was turned off (keeping the element stiffness limited by the failure surface without eliminating the element totally at the crushing state).

2.2.3. Application of loads and numerical control

The loads were incrementally applied to the model using the load control strategy applying the Newton–Raphson procedure. Forces convergence criterion is considered throughout the analysis. The tolerance associated with this convergence criterion and the load step increments are varied in order to solve potential numerical problems. The load control strategy is adopted due to the existence of several applied loads.

2.2.4. Boundary conditions

In the 3D model studied herein, boundary conditions are used to imply symmetric behavior in x- and z-directions so that the model size is quartered (Fig. 6). Hence, all nodes along the surface of the stub girder at mid-span (surface 1) are restricted from moving in the x-direction due to symmetry. Moreover, all nodes of the middle surface (surface 2) of the stub girder section are restricted from moving in the z-directions, where local buckling in webs of both stubs and main girder is prevented.

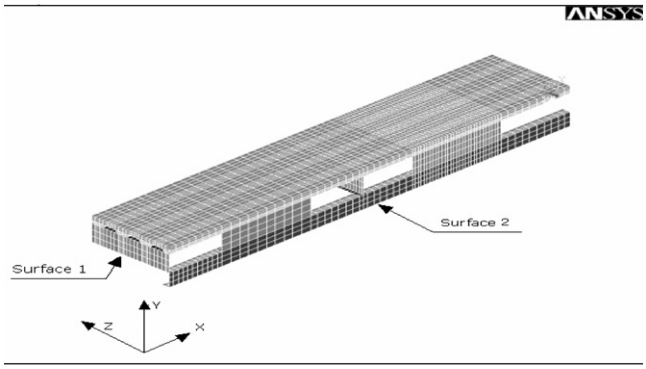

Figure 6 The surfaces of symmetry in the 3D model.

All coincident nodes at the interface between the concrete slab and the stub flanges are coupled in the y- and z-directions only allowing slip in x-direction, while the coincident nodes at the interface between the concrete slab and the secondary beams were coupled in the y- and x-directions only allowing slip in z-direction. The nodes at the support are restricted from moving in the y- and z-directions.

3. Verification of the proposed finite element models

The proposed two and three-dimensional finite element models are verified and compared with the experimental and the numerical results available in the literature. The 2D model is verified through the simulation of the overall flexural behavior of four stub girders. The first three girders namely, SG5, SG6 and SG7, as reported by Wang et al. [18], are simply supported and subjected to a concentrated load applied in the mid-span. In these girders, full interaction between the concrete slabs and the stubs is assumed. The fourth girder namely, BJOR, as carried out by Bjorhovde and Zimmerman [3], is a simply supported stub-girder subjected to three points of loads. The relevant geometrical and material properties of all girders are

Table 1 Geometrical and material properties of the verified stub girders.

Stub girder	Total span, L (m)	Main girder			Stub		Open panel length, $2a$ (mm)	Concrete slab			
		Section	f_{yf} (MPa)	f_{yw} (MPa)	Section	Numbers	Length	b Effective width of concrete slab (mm)	d Effective depth of slab (mm)	d_1 Concrete cover (mm)	f_c Cylinder strength of concrete (MPa)
SG5	3.66	W6 × 15.5	323.7	336.3	S5 × 10	5	305	533.8	406.4	82.6	19	30.18
SG6	3.66	W6 × 15.5	323.7	336.3	S6 × 12.5	5	305	533.8	406.4	82.6	19	31.01
SG7	3.66	W6 × 15.5	323.7	336.3	S8 × 18.4	5	305	533.8	406.4	82.6	19	29.00
BJOR	13.4	W310 × 86	323.7	336.3	W410 × 39	4	1525	1748	2680	120	40	30.18

summarized in Table 1. The 3D model is verified through the simulation of the overall flexural behavior of the stub-girder, BJOR.

3.1. 2D model for full interaction stub-girders (SG5, SG6 and SG7)

In general the results of the proposed finite element model using ANSYS [2], shown in Figs. 7–9 are in good agreement with the experimental results [18] and the FEM package ABAQUS results by Wang et al. [18]. The results obtained show that the results of the proposed finite model are conservative when approaching the ultimate load in stub girders SG5 and SG7. The results of the numerical model PZA [9,10] are conservative until the ultimate load, then the results became non-conservative, except for the stub girder SG7 where the results of PZA were in excellent agreement with the experimental results.

3.2. 2D model for partial interaction stub-girder (BJOR)

As shown in Fig. 10, good agreement between the test results [3] and the results of the presented 2D model is shown but the present model gave slightly higher results than the experimental results in the plastic range (11% difference in the ultimate load). This may be attributed to the use of assumed load–

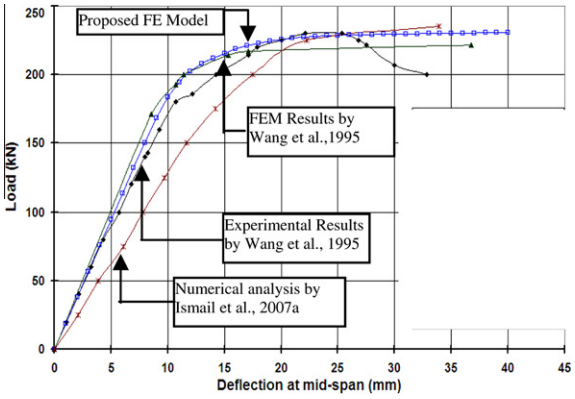

Figure 7 Load–deflection curves for stub girder (SG5).

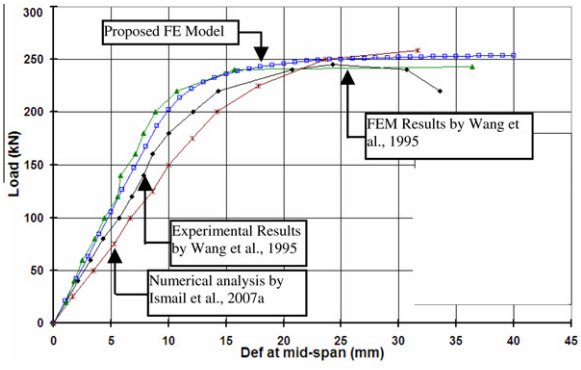

Figure 8 Load–deflection curves for stub girder (SG6).

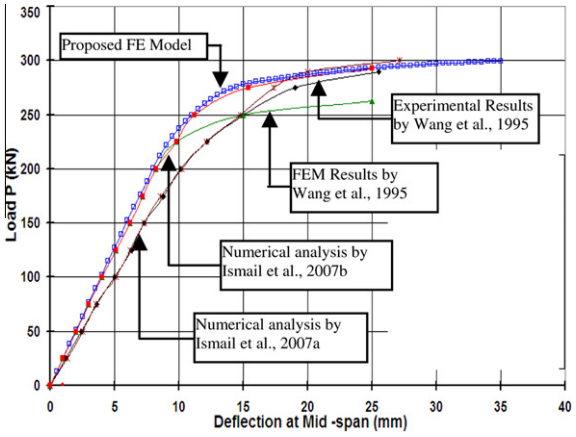

Figure 9 Load–deflection curves for stub girder (SG7).

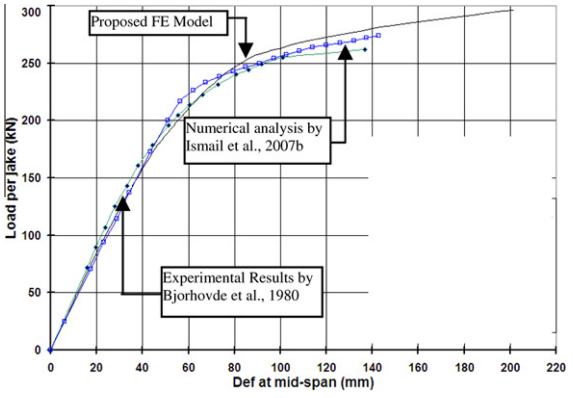

Figure 10 Load–deflection curves for stub girder (BJOR).

slip curve for the shear connectors rather than the real one which was not available by the experimental work.

A previous research [11] presented an FE model in 2D using COSMOS software. The proposed model takes into consideration the nonlinear behavior of all materials and the effect of partial composite action by modeling the stud as an elastic–plastic beam element ignoring the nonlinear response of the shear connectors. This model was validated by comparison against the test results [3]. The results of the present 2D model using ANSYS [2] are compared with the published results of COSMOS where good agreement between the two models is achieved as shown in Fig. 10.

3.3. 3D model for partial interaction stub-girder (BJOR)

As shown in Fig. 11, good agreement between the 3D model and the test results is achieved till approaching the ultimate load where the 3D model fails to continue and stopped earlier with slightly higher ultimate load and smaller corresponding deflection. This is attributed to the numerical divergence problems associated with the occurrence of cracks in the concrete slab (when the cracks are not considered, the 3D model has the ability to continue).

Based on the investigation of the proposed models, it is clear that the load–deflection curves obtained by both the 2D model and the 3D model are identical as shown in Fig. 12. Moreover, the run-time and the storage space required for the 2D analysis are much less than those for the 3D one.

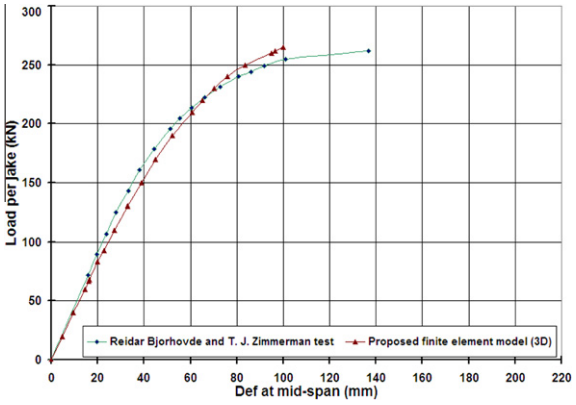

Figure 11 Verification of the 3D model with Bjorhovde's experimental results.

Accordingly, the 2D model is selected for extensive parametric study of stub girder, avoiding meshing difficulties, memory requirements, time consuming and numerical divergence problems.

4. Parametric study

4.1. Effect of material properties

In this section, an investigation is performed to assess the sensitivity of the overall response of stub girder (represented by the load–deflection curve including the elastic stiffness, the strength and the ductility factor which are calculated according to AISC [1]) to likely variations in material strengths considering concrete strength and steel strength.

4.1.1. Influence of concrete strength

Concrete strengths of 25–40 MPa are most common [4], although the choice also depends on the limit state of the stud shear connectors. This parameter will be studied through the use of different concrete compressive strengths in the slab and in the associated push-out tests represented by the load–slip curves of shear connectors. The load–slip curves of the

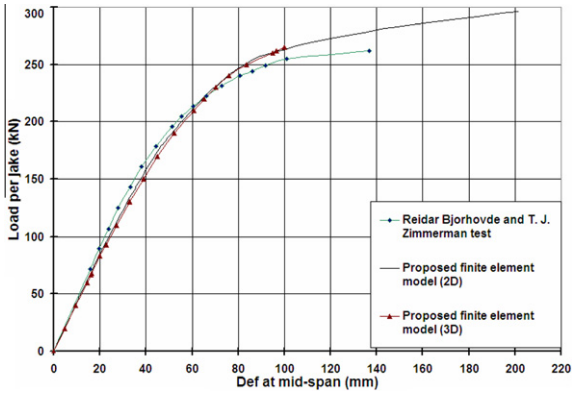

Figure 12 Comparison between the 2D and the 3D model of Bjorhovde's experiment.

shear connectors used in this parametric study for different concrete strengths (25 and 40 MPa) are shown in Fig. 13. It is noticeable that the strengths of these shear connectors are controlled by the concrete strength only whereas the other parameters of shear connectors were constant.

The effect of the concrete strength is investigated, where the variation in concrete slab strength is done in conjunction with variation in concrete strength for push-out specimen. The load versus mid-span deflection curves for different concrete strengths (25 and 40 MPa) are shown in Fig. 14. It appears that the concrete slab strength variation has almost no influence on the elastic stiffness and strength, while an increase of 29% in ductility is achieved with increase in the concrete strength.

4.1.2. Effect of steel strength

In this study, the effect of the variation of steel strength (represented by the variation in the value of yield stress only) utilized in the steel components of stub girder will be investigated.

4.1.2.1. Effect of steel strength ofall steel components. As shown in Fig. 15, the variation of steel strength of all steel components (main girder and stubs) is very effective in improving the behavior of the stub girder in the plastic stage (the start of yielding and the value of ultimate load), while there is no change in the initial stiffness which depends on the constant modulus of elasticity. Accordingly, there is an improvement

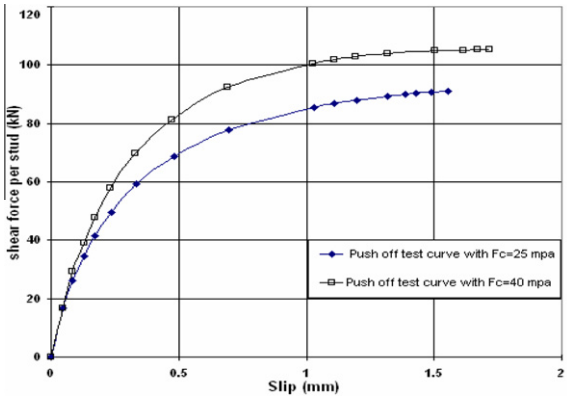

Figure 13 The load–slip curves of the shear connector for different concrete strength.

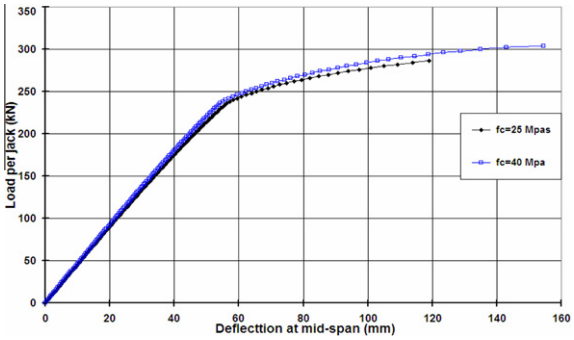

Figure 14 The load versus mid-span deflection curves with variation of the concrete strength.

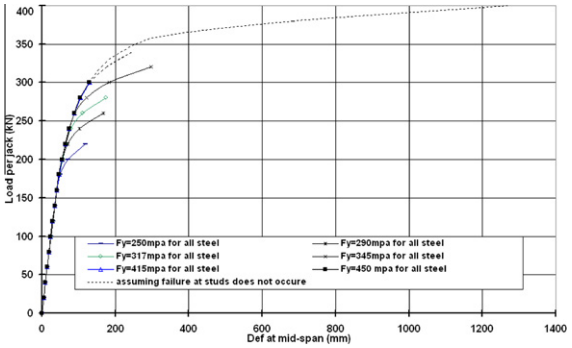

Figure 15 Load–deflection curves for variations in steel strength of all components of stub-girder floor system.

in the stub girder strength with the increase of steel strength of all steel components with steel strength up to 345 MPa where the failure of stub girder is controlled by the steel strength (for this particular dimension of stub girder where it is designed according to assumption that the failure will start first in the steel main girder [19]), while beyond this limit the strength of stub girder is controlled by the shear connector failure (Fig. 17).

4.1.2.2. Effect of steel strength of main girder. The steel strength of main girder is varied while the steel strength of stub components is kept constant. As can be seen in Fig. 16, the steel strength of the main girder plays an important role where an improvement in the behavior of the stub girder in the plastic range is achieved with steel strength of main girder up to 415 MPa. After this limit the strength of the stub girder is constant. To improve the strength of the stub girder (BJOR), the increase of steel strength used in all steel components is the best choice with steel strength up to 345 MPa, while beyond this limit the increase of steel strength used in the main girder is the best choice for this specific stub girder, as shown in Fig. 17.

4.2. Effect of relative dimensions

In this section, a study is performed to investigate the effect of several parameters, related to the layout of floor system, on the overall behavior of stub-girder floor system. The parameters studied herein are concrete slab depth, height of main girder,

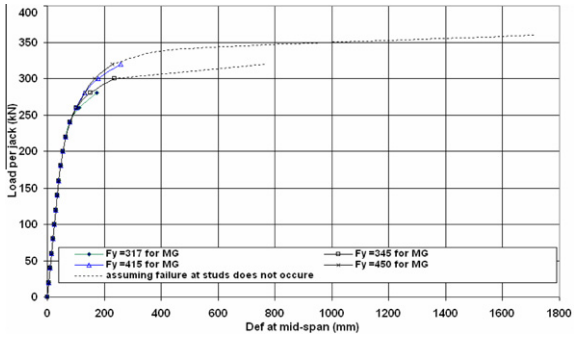

Figure 16 Load–deflection curves for variations in steel strength of main girder.

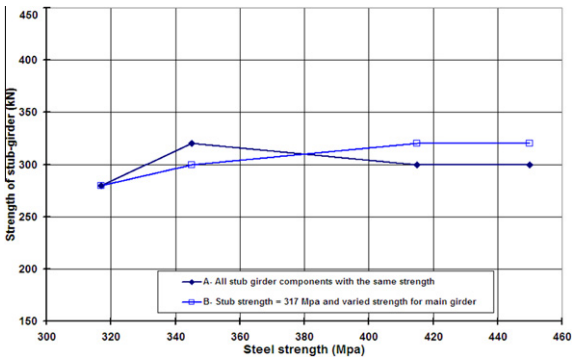

Figure 17 Strength of stub-girder with variation in steel strength of stub-girder floor system.

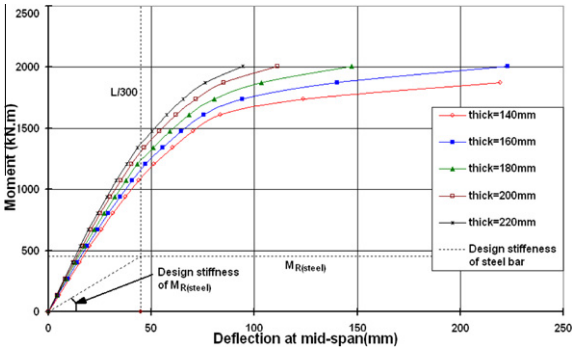

Figure 18 Moment–deflection curves for variations of slab depth for main-girder section W12 × 58.

height of stub-to-height of main girder ratio and finally the length of exterior stub.

4.2.1. Effect of the concrete slab depth

The effect of variation of the concrete slab depth is studied with several main girder sections (W12 × 58, W16 × 77 and W21 × 101), where the results are shown in Figs. 18–20. We notice that when the depth is increased, there is a good improvement in the overall behavior of stub girder shown through an increase in the stiffness for all studied main girders and an increase in the moment capacity for relatively large main girder sections. This is expected as an increase in the slab

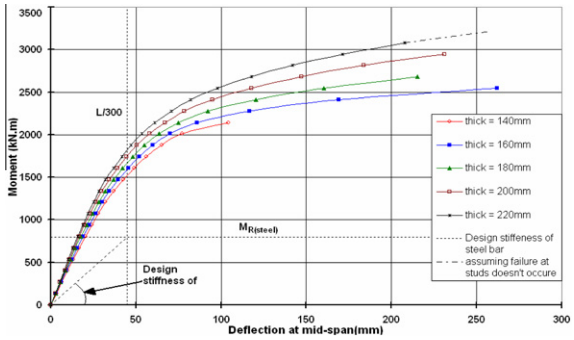

Figure 19 Moment–deflection curves for variations in slab depth for main-girder section W16 × 77.

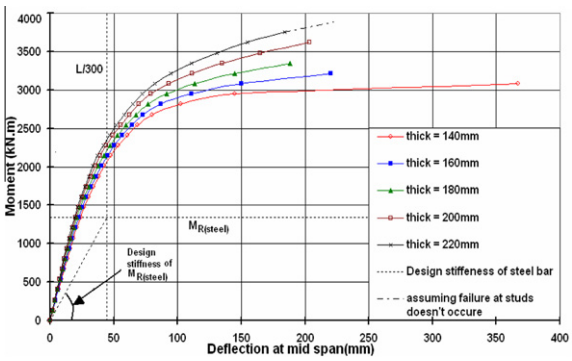

Figure 20 Moment–deflection curves for variations in slab depth for main-girder section W21 × 101.

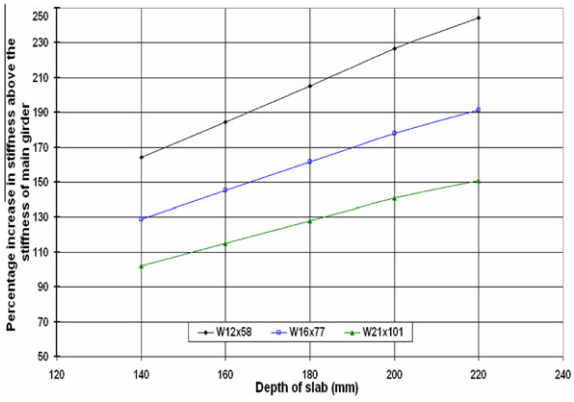

Figure 21 Percentage increase in stiffness above the stiffness of main-girder for variations in slab depth and steel section.

depth would raise the neutral axis of the stub girder, hence increasing the lever arm of the section.

As shown in Fig. 21, the stiffnesses of the stub girders are increased by 164.26%, 184.36%, 205.22%, 226.56%, and 244.4% of the stiffness of the used main girder (W12 × 58) when using 140, 160, 180, 200, and 220 mm concrete slabs, respectively.

As the steel section of main girder becomes comparatively deeper, the effect of the concrete slab depth becomes less significant as the stiffnesses of the stub girders are increased by129%, 145%, 161.52%, 177.9%, and 191.35% of the stiffness of the main girder of W16 × 77 section, while these values are 102%, 115.1%, 128.2%, 140.86%, and 150.85% in case of main girder of section W21 × 101.

Moreover, Fig. 22 shows the variation of the moment capacity ratio, $M_R/M_{R(steel)}$, for variations in the slab depth and main-girder section, where $M_{R(steel)}$ is the plastic moment capacity of the fully restraint steel beam. The study shows an increase in the moment capacity of stub girder with the increase in concrete slab depth for relatively large main girder sections, while for typical main girder section (W12 × 58) the effect of the increase in concrete slab depth over the typical value (160 mm) is null, where the increase of the concrete slab depth becomes inefficient with relatively small main girders as the behavior is controlled by the main girder.

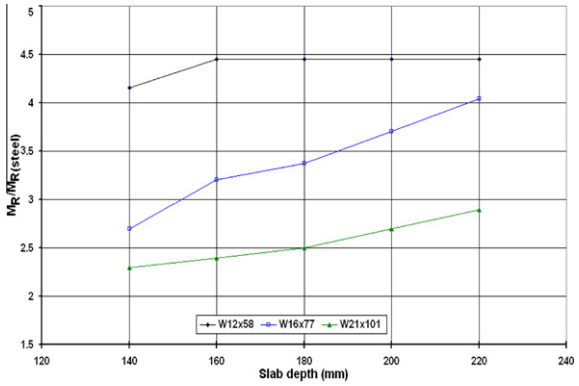

Figure 22 Moment capacity ratio, $M_R/M_{R(steel)}$ for variations in slab depth and main-girder section.

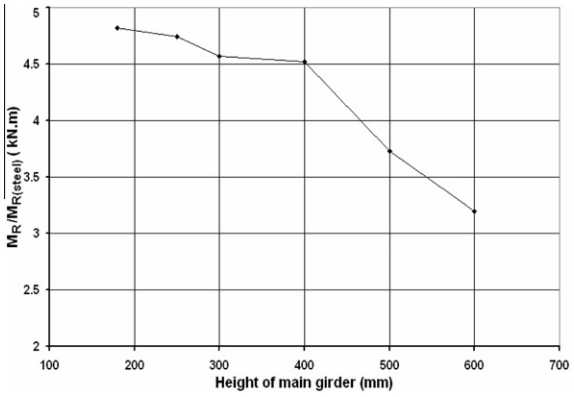

Figure 24 The moment capacity ratio, $M_R/M_{R(steel)}$ for variations of main girder height.

4.2.2. Effect of change in height of main girder

To study the effect of change in height of main girder, the overall height of stub girder-to-span ratio is changed from 11.57 to 18.14 while other parameters were kept constant (the concrete slab depth and the section of stubs). With respect to the main girder, the flange width, flange thickness and web thickness are kept constant (180, 15 and 12 mm, respectively). These values are taken for all stub girders to keep the main girder in classification of compact section, H_w/t_w and $(B_f/2)/t_f$, where H_w is the depth of the web, t_w is the thickness of the web, B_f is the width of the flange and t_f is the thickness of the flange, are conformed to the standard American sections, where the local web buckling does not reduce the plastic strength of the main girder if the beam depth-to-web thickness ratio is not larger than $3.76\sqrt{E/f_y}$, where E is the modulus of elasticity and f_y is the yield stress of steel, according to AISC [1]. So each height of stub girder is investigated on the assumption that no local failure would prevent the bottom chord from reaching its ultimate capacity.It is clear that the increase in the main girder height will increase the resistant moment, M_R and stiffness of the stub girder as shown in Fig. 23. However, it is worth noting that the value of $M_R/M_{R(steel)}$ ratio reduces with the increase of the main girder height, Fig. 24, where the moment capacity of main girder increases more rapidly than the overall moment capacity of stub girder with the increase in the main girder height, hence the composite action is less efficient with relatively large steel sections.

Also in Fig. 25, the stiffness of the stub girder is increased by 288%, 241%, 223%, 198%, 185% and 180% of the stiffness of the main girder with main girder heights 180, 250, 300, 400, 500 and 600 mm, respectively.

4.2.3. Effect of height of stub-to-height of main girder ratio

In this parameter, height of stub-to-height of main girder ratio is varied (this ratio is taken as 0.75, 1.0, 1.25, 1.50) while the overall height of stub-girder system and the other parameters are kept constant. It means that when this ratio increases the height of main girder decreases. Moreover, this parameter is studied for different slab depths (160, 180 and 200 mm). As shown in Fig. 26, the resistance and the ductility factor are almost constant, for the stub girders with 160 mm slab depth, with ratios range from 0.75 to 1.25 while there is no significant decrease in the stiffness for these ratios as shown in Fig. 29. At stub height-to-main girder height ratio 1.5, the resistance and ductility factor decreased by 6% and 17%, respectively. Also Fig. 27 shows the same observation, for stub girders with slab depth of 180 mm, but the resistance decreases by 12.5% and the ductility factor decreases by 25% for the ratio of 1.5, respectively. As can be seen in Fig. 28, the response of stub girder becomes more sensitive to the ratio of height of stub-to-height of main girder with 200 mm slab depth where the resistance and the ductility factor decrease with the increase of that ratio. Figs. 30 and 31 show the variation in strength and duc-

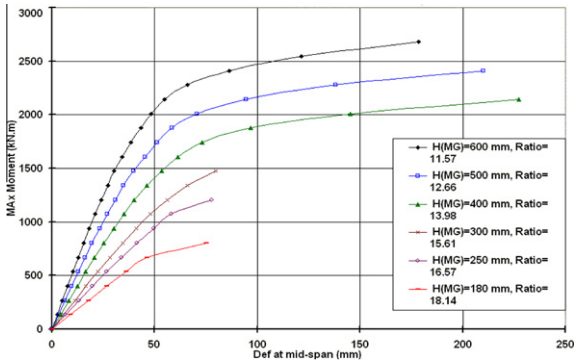

Figure 23 Moment–deflection curves for variations in main girder height.

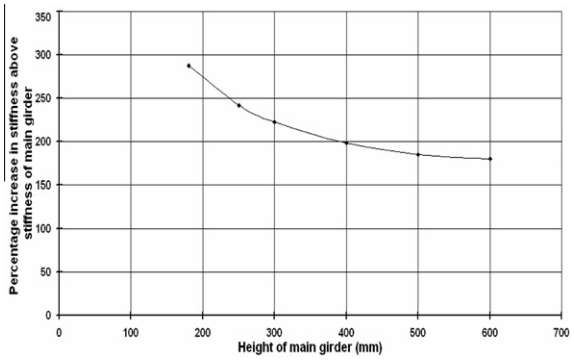

Figure 25 Percentage increase in stiffness above the stiffness of main girder for variations in girder height.

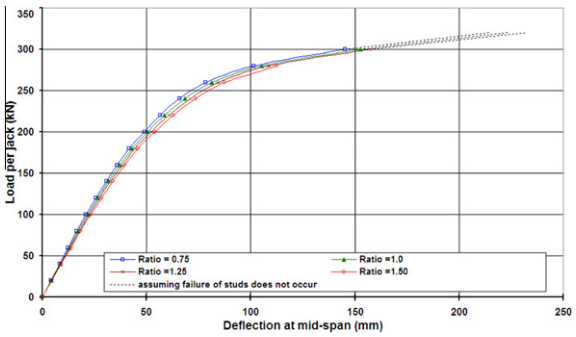

Figure 26 Load–deflection curves for variations in stub height-to-main girder height ratio for 160 mm slab depth.

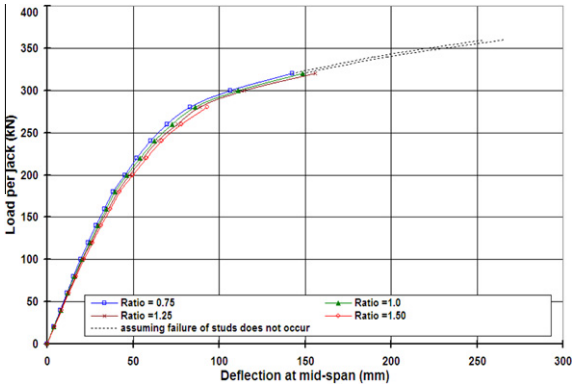

Figure 27 Load–deflection curves for variations in stub height-to-main girder height ratio for 180 mm slab depth.

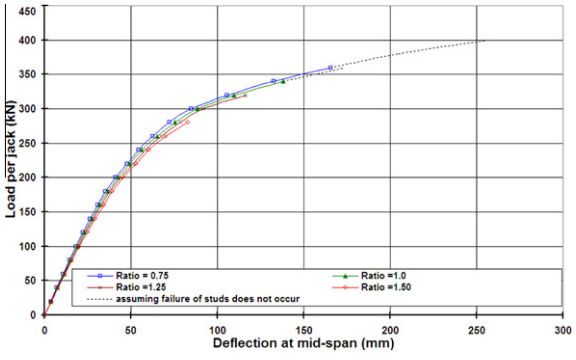

Figure 28 Load–deflection curves for variations in stub height-to-main girder height ratio for 200 mm slab depth.

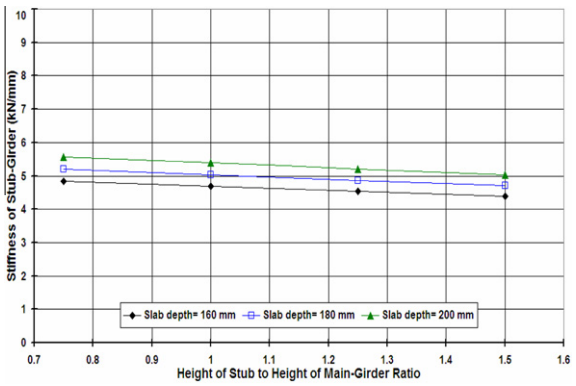

Figure 29 Stiffness of stub-girder for variation in stub height-to-main girder height ratio and slab depth.

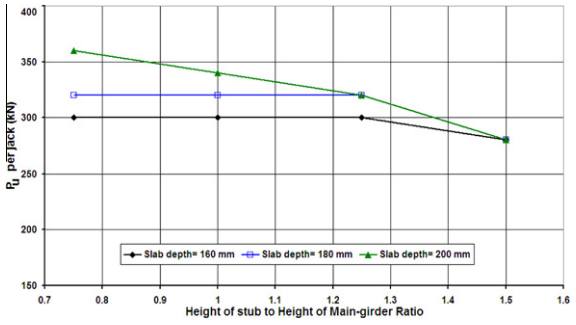

Figure 30 Strength of stub-girder for variation in stub height-to-main girder height ratio and slab depth.

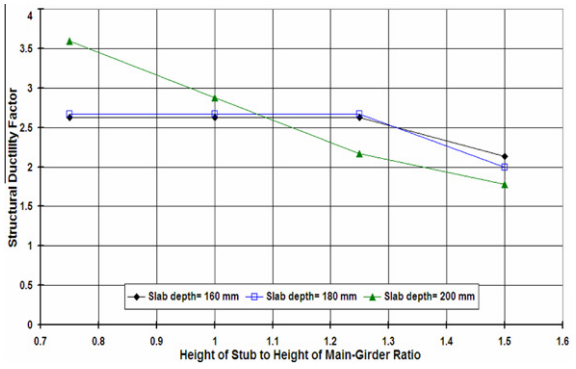

Figure 31 Structural ductility factor of stub-girder for variation in stub height-to-main girder height ratio and slab depth.

tility factor of stub-girder for variation in stub height-to-main girder height ratio and slab depth.

Accordingly, it can be concluded that "*the efficient ratio*" of stub height-to-main girder height is 1.25 for concrete slab depths (160 and 180 mm), while this ratio decreases to 0.75 with the increase of concrete slab depth to 200 mm.

The effect of this parameter can be explained as follows: as the stub height-to-main girder height ratio increases, the main girder stiffness decreases while the lever arm increases. Both the decrease in the main girder stiffness (both axial stiffness and bending stiffness) and the increase in the lever arm balance with each other, leading to almost constant stub girder strength and ductility in addition to small decrease in the stiffness, for stub height-to-main girder height ratios lower than a certain value named as *the efficient ratio*. For stub height-to main girder height ratios higher than the efficient ratio, the decrease in the main girder stiffness reaches a critical value that controls failure. This *efficient ratio* decreases with the increase of concrete slab depth where failure is controlled by the main girder, allowing the effect of the stub height-to-main girder height ratios, higher than the efficient ratio, to be dominant.

4.3. Effect of the length of exterior stub

In this section, the effect of the length of the exterior stub is investigated where this effect controls the behavior of stub girders as will be shown. That is, the stubs are loaded primarily in shear, which explains why the interior stubs can be kept so much shorter than the exterior ones. As a practical guideline [19,4], the exterior stubs are normally 5–7 ft long but in the present study the length of exterior stub is varied from 3 to 8 ft, using the same spacing for shear connectors. The length of exterior stub is increased by decreasing the exterior open width. This study is implemented with variation of the height of main girder (180, 250, 300, 400, 500 and 600 mm) and other parameters are kept constant.

The moment–deflection curves, with variation in the exterior stub length for various main girder heights, are plotted in Figs. 32–35. These curves show a marked improvement in the overall response for all heights of main girder due to an increase in the length of exterior stub. Fig. 36 shows an average increase in the stub girder resistance 33.6% for each foot increase in the exterior stub length up to exterior stub 7 ft long, beyond which full composite action could be achieved. Moreover, Fig. 37 shows an increase in the stiffness of the stub girder by increasing the length of exterior stub.

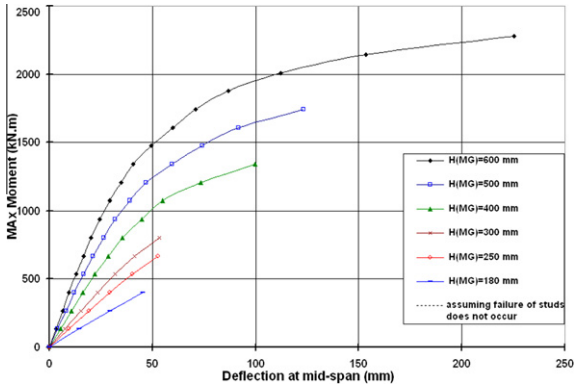

Figure 32 Moment–deflection curves for variations in stub girder height for exterior stub with length 3 ft.

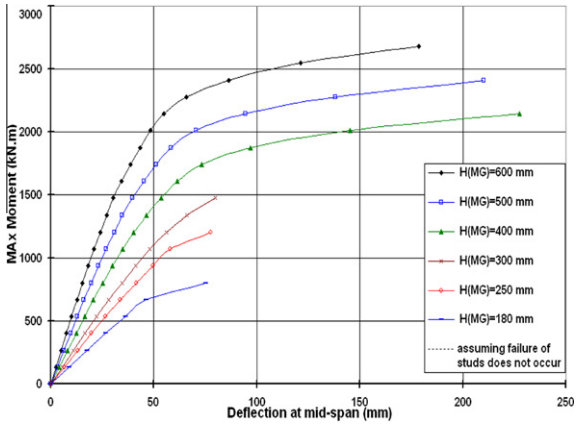

Figure 33 Moment–deflection curves for variations in stub girder height for exterior stub with length 5 ft.

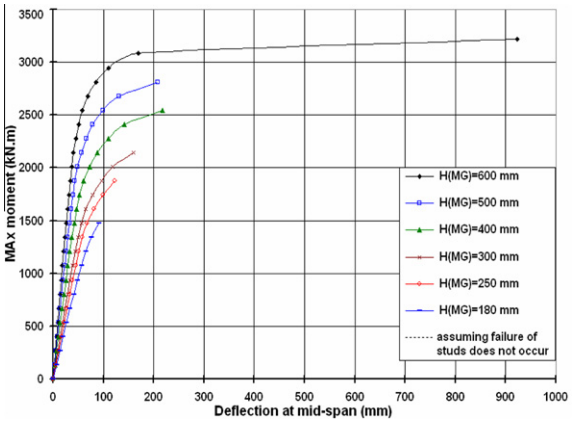

Figure 34 Moment–deflection curves for variations in stub girder height for exterior stub with length 7 ft.

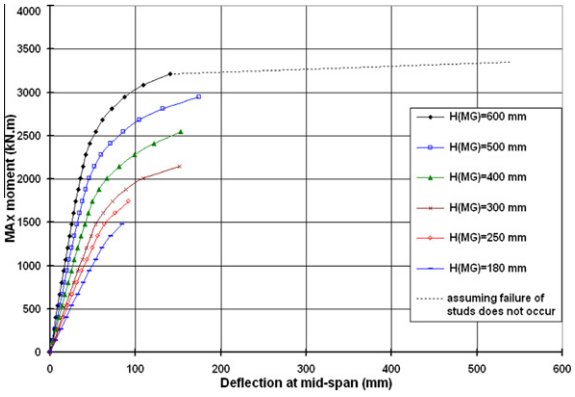

Figure 35 Moment–deflection curves for variations in stub girder height for exterior stub with length 8 ft.

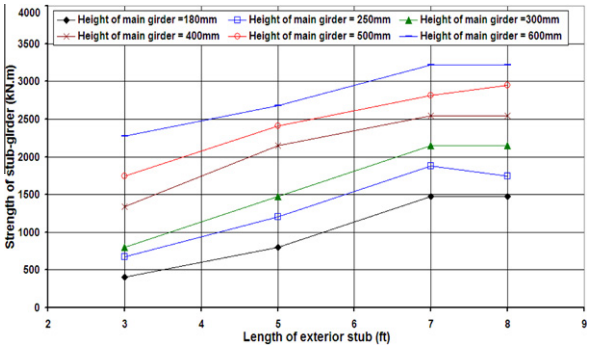

Figure 36 Resistance of stub girders with variations in exterior stub length and height of main girder.

From the previous figures, it is worth noting that for stub girder with 250 mm main girder height with 7 ft exterior stub length can provide higher resistance than that of the stub girder with 300 mm main girder height and 5 ft exterior stub length with the same stiffness. Therefore, more economical sizing of the main girder can be achieved with an increase of the exterior stub length. This improvement in the resistance and

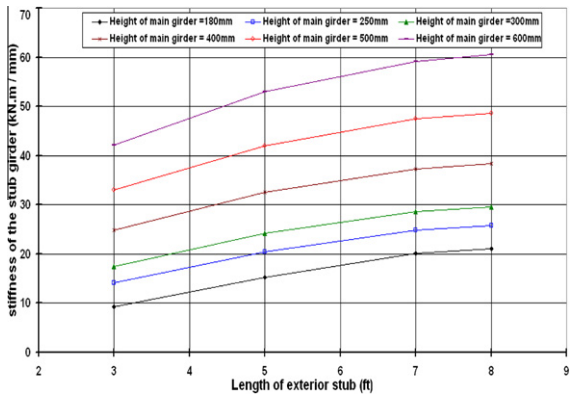

Figure 37 Stiffness of the stub girder with variations in the length of exterior stub and the main girder height.

stiffness due to an increase in the exterior stub length can be attributed to the increase in the shear force transferred by the exterior stub which helps to develop more composite action between the concrete slab and the main girder.

Finally, it is worth noting that the section at the exterior end of exterior stub is one of the three potentially governing sections of the girder as well as the sections at the mid-span and at the exterior end of interior stub [3,19,4]. This fact can be used as an additional reason to justify the improvement in the resistance of stub girder which occurs with the increase in the exterior stub length, leading to a decrease in the length of exterior open width.

4.4. Effect of shear connector characteristics

In this section, the effect of shear connector stiffness and the effect of stud spacing are studied.

4.4.1. Effect of stiffness of shear connector

The influence of the shear connector stiffness is studied considering different stud stiffnesses. These stiffnesses (k) are taken as a ratio (0.5, 1.5, 2, 2.5, 5 and 10) of the stiffness (k_0) of the shear connector used for BJOR stub girder.

As shown in Fig. 38, it is worth noting that the increase in the stiffness of studs is associated with the increase in stud resistance.

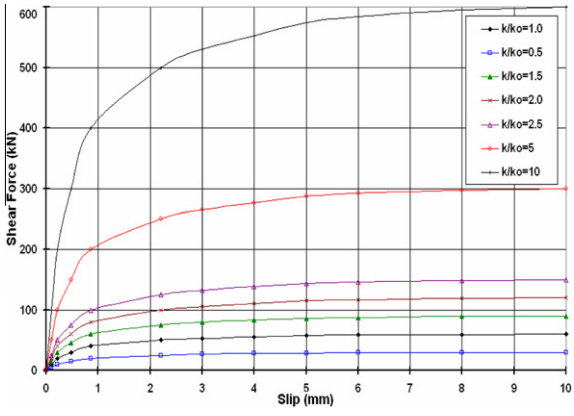

Figure 38 Load–slip curves with different stud stiffness.

The numerical results for different stiffness values are shown in Fig. 39 which confirms that the stiffness of the shear connector is a main factor in the composite action that raises the resistance and the stiffness of the stub girder system. As shown from Fig. 39, there is a certain value of stud stiffness (k/k_0 = 1.0 in this studied case) after which the stub girder resistance becomes constant while the increase in the stub girder stiffness is very small, Fig. 40, where full composite action is almost achieved.

4.4.2. Effect of the shear connector spacing at exterior stub

To investigate the effect of spacing of shear connectors at the exterior stub, the number of shear connectors distributed along the exterior stub is varied (15, 10, and 5 pairs of studs). In Fig. 41, the load–deflection curves confirm that as the number of the studs at exterior stub decreases, the stub girder strength decreases where the total horizontal shear force transferred throughout the stub decreases, weakening the composite action. As shown in Fig. 42, it is clear that when the number of studs at the exterior stub is the typical number considering the design formulas [19] (15 pairs of studs), the stub girder failure does not occur due to stud failure though care must be taken for studs of interior stub where the stud forces are bigger

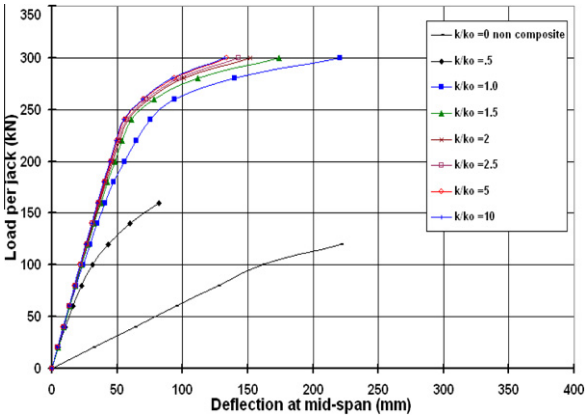

Figure 39 Load–deflection curves for different load–slip curves of shear connectors.

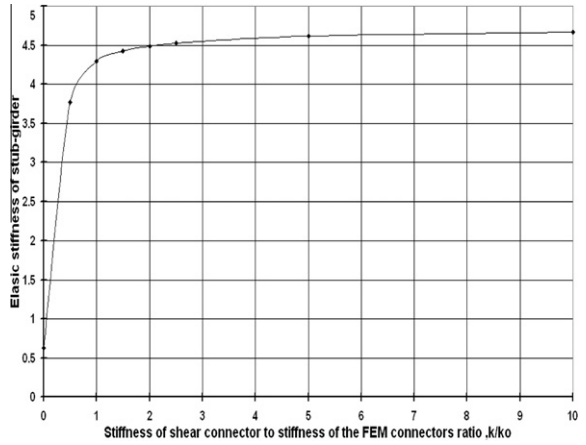

Figure 40 Initial stiffness of stub girder with variation in stiffness of shear connectors.

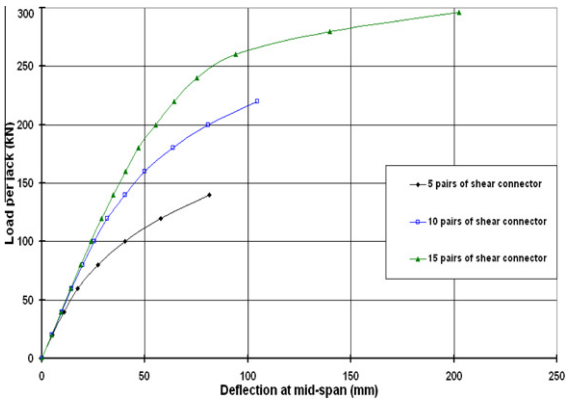

Figure 41 Load–deflection curves for variations in spacing of shear connectors at exterior stub.

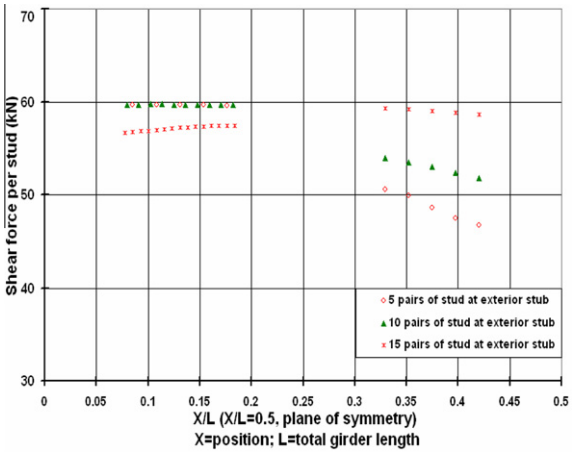

Figure 42 Shear force of studs along the stub girder at the ultimate load for variations in spacing of shear connectors at the exterior stub.

than those of exterior stub. When the number of studs is decreased, the stub girder failure occurs due to the failure of studs at the exterior stub.

In this context it is important to observe that the shear force distribution is almost constant along the length of both of the exterior and interior stubs, leading to distribute the shear connectors uniformly along the length of the stubs.

5. Conclusions

Analytical two and three dimensional finite element models have been developed in order to study the behavior of composite stub-girders with full and partial shear connection. From the analyses performed for the stub-girder floor system in two and three dimensions, the following conclusions are drawn:

(1) The results obtained from the 2D model, for the stub girders with full and partial shear connection, are in good agreement with the previous experimental and numerical results.
(2) The results obtained from the 3D model, for the stub girder with partial shear connection, exhibit good correlation with the available experimental results in the literature till approaching the ultimate load where the 3D model failed to continue and stopped earlier with slightly higher ultimate load and smaller corresponding deflection. This is attributed to the numerical divergence problems associated with the occurrence of cracks in the concrete slab. Moreover, it was noticed that if the crushing capability of the concrete is turned on (the elastic modulus is set to zero in all directions of the crushed element so the element effectively disappears), the finite element model fails prematurely where the crushed concrete elements significantly reduce the local stiffness. Therefore, in the study of such type of floor system, the crushing capability is turned off (keeping the element stiffness limited by the failure surface without eliminating the element totally at the crushing state). This strategy is justified because the crushed elements in the concrete slab as approaching the ultimate load are very few, while cracking of the concrete is enabled whereas large number of cracked elements in the concrete slab is found along the main girder at failure.
(3) Based on the investigation of the proposed models, it is clear that the load–deflection curves obtained by both the 2D model and the 3D model are identical. Accordingly, the 2D model is recommended for the parametric study.
(4) The variation of the concrete strength in both the push-out test and concrete slab has a small influence on the behavior of stub girder, whereas there is almost no difference in the elastic stiffness and strength, while increase in ductility is achieved with increase in the concrete strength.
(5) With the increase of the concrete slab depth, there is a good improvement in the overall behavior of stub girder shown through an increase in the stiffness for all studied main girders and an increase in the moment capacity for relatively large main girder sections only, where the increase of the concrete slab depth becomes inefficient with relatively small main girders as the behavior is controlled by the main girder.
(6) There is an *efficient ratio* of stub height-to-main girder height under which there is almost no change in the stub girder strength and ductility with the increase of the stub height-to-main girder height ratio, while there is small decrease in stiffness. For an increase in stub height-to-main girder height ratios, higher than the efficient ratio, the stub girder strength and ductility decrease significantly with small decrease in stiffness. The *efficient ratio* of stub height-to-main girder decreases with the increase of concrete slab depth.
(7) It can be concluded that more economical sizing of the main girder can be obtained with increasing the exterior stub length. An average increase in the stub girder resistance 33.6% for each foot increase in the exterior stub length is achieved up to exterior stub 7 ft long. Moreover, an increase in the stiffness of the stub girder is obtained by increasing the length of exterior stub.
(8) There is a certain value of stud stiffness, for each studied case, after which the stub girder resistance becomes constant while the increase in the stub girder stiffness is very small, where full composite action is almost achieved.

(9) When the number of studs at the exterior stub is the typical number considering the design formulas, the stub girder failure does not occur due to stud failure. When the number of studs is decreased, the stub girder failure occurs due to the failure of studs at the exterior stub. Also, it is important to observe that the shear force distribution is almost constant along the length of both of the exterior and interior stubs, supporting the common practice to distribute the shear connectors uniformly along the length of the stubs.

References

[1] American Institute of Steel Construction (AISC), LRFD Specification for Structural Steel Buildings, December 27, 1999.

[2] ANSYS, Swanson Analysis Systems Online Manual, Version 10.0, and Theory Reference.

[3] R. Bjorhovde, T.J. Zimmerman, Some aspects of stub girder design, AISC Eng. J. 17 (3) (1980) 54–69.

[4] R. Bjorhovde, Stub girder floor systems, in: Wai-Fah Chen (Ed.), Structural Engineering Handbook, CRC Press LLC, Boca Raton, 1999.

[5] D.J. Carreira, K.H. Chu, Stress–strain relationship for concrete in compression, ACI J. 82 (11) (1985) 797–804.

[6] J.P. Colaco, A stub girder system for high-rise buildings, AISC Eng. J. 9 (2) (1972) 89–95.

[7] J.P. Colaco, Partial tube concept for mid-rise structures, AISC Eng. J. 11 (4) (1974) 81–85.

[8] M.M. Harbok, M.U. Hosain, Analysis of stub-girder using sub structuring, Comput. Struct. 8 (1978) 615–619.

[9] R.S. Ismail, M.T. El-Katt, H.A. Zien El Din, Y.M. Kasem, Behavior of multi-layer composite stub-girder. Part I: inelastic analytical model, in: Sixth International Alexandria Conference on Structural and Geotechnical Engineering, Alexandria, Egypt, ST-87, 15–17 April, 2007.

[10] R.S. Ismail, M.T. El-Katt, H.A. Zien El Din, Y.M. Kasem, Behavior of multi-layer composite stub-girder. Part II: finite element model, in: Sixth International Alexandria Conference on Structural and Geotechnical Engineering, Alexandria, Egypt, ST-107, 15–17 April, 2007.

[11] Y.M. Kasem, Analysis of Multi-Layer Composite Beams Ultimate Strength Analysis of Stub-Girder, M.Sc., Alexandria University, Faculty of Engineering, Egypt, 2005.

[12] D. Lam, K.S. Elliott, D.A. Nethercot, Experiments on composite steel beams with precast concrete hollow core floor slabs, Proc. Inst. Civil Eng. Struct. Build. 140 (2) (2000) 127–138.

[13] Mohd S.Z. Madros, The Structural Behavior of Composite Stub-Girder Floor Systems, Ph.D., Darwin College, The University of Cambridge, November, 1989.

[14] F.D. Queiroz, P.C.G.S. Vellasco, D.A. Nethercot, Structural assessment of composite beams using the finite element method, in: Eurosteel Conference of Steel and Composite Structures, Eurosteel05, vol. B, 2005, pp. 4.3-49–4.3-58.

[15] F.D. Queiroz, P.C.G.S. Vellasco, D.A. Nethercot, A non-linear evaluation of steel–concrete composite beams by the finite element method, in: Fourth International Conference on Advances in Steel Structures, 2005, pp. 88–102.

[16] F.D. Queiroz, P.C.G.S. Vellasco, D.A. Nethercot, Finite element modeling of composite beams with full and partial shear, J. Constr. Steel Res. 63 (2007) 505–521.

[17] D.M. Stuart, Antiquated Structural Systems Series-Structural Steel Composite Stub-Girder Construction, Part 6, Structure Magazine, November, 2008.

[18] C.M. Wang, K. Padmanaban, N.E. Shnanmagom, Ultimate strength analysis of stub-girders, ASCE J. Struct. Eng. 121 (9) (1995) 1259–1264.

[19] T.J. Zimmerman, R. Bjorhovde, Analysis and Design of Stub Girders, Structural Eng. Report, No. 90, University of Alberta, Edmonton, Alberta, Canada, March, 1981.